HHS Public Access

Author manuscript

Cell Rep. Author manuscript; available in PMC 2019 March 06.

Published in final edited form as:

Cell Rep. 2019 February 19; 26(8): 2178–2193.e3. doi:10.1016/j.celrep.2019.01.085.

Mass Cytometry Analysis Reveals that Specific Intratumoral CD4+ T Cell Subsets Correlate with Patient Survival in Follicular Lymphoma

Zhi-Zhang Yang[1,3,*], **Hyo Jin Kim**[1], **Jose C. Villasboas**[1], **Tammy Price-Troska**[1], **Shahrzad Jalali**[1], **Hongyan Wu**[2], **Rebecca A. Luchtel**[1], **Mei-Yin C. Polley**[1], **Anne J. Novak**[1], and **Stephen M. Ansell**[1,*]

[1]Division of Hematology and Internal Medicine, Mayo Clinic, Rochester, MN, USA

[2]Department of Immunology, Medical College, China Three Gorges University, Yichang, Hubei, China

[3]Lead Contact

SUMMARY

Follicular lymphoma (FL) is an indolent B cell malignancy characterized by an extensive but poorly functional T cell infiltrate in the tumor microenvironment. Using mass cytometry, we identified at least 12 subsets of intratumoral $CD4^+$ T cells, 3 of which were unique to FL biopsies versus control tissues. Of these subsets, the frequency of naive T cells correlated with improved patient survival. Although total $PD\text{-}1^+$ T cell numbers were not associated with patient outcome, specific $PD\text{-}1^+$ T cell subpopulations were associated with poor survival. Intratumoral T cells lacking CD27 and CD28 co-stimulatory receptor expression were enriched in FL and correlated with inferior patient outcomes. *In vitro* models revealed that $CD70^+$ lymphoma cells played an important role in expanding this population. Taken together, our mass cytometry results identified $CD4^+$ memory T cell populations that are poorly functional due to loss of co-stimulatory receptor expression and are associated with an inferior survival in FL.

In Brief

Yang et al. utilize mass cytometry (CyTOF) to characterize intratumoral T cells and explore the clinical relevance of T cell subsets in follicular lymphoma (FL). Clustering analysis reveals an immune signature with reduced expression of co-stimulatory molecules on intratumoral T cells that correlated with a poor prognosis in FL.

*Correspondence: yang.zhizhang@mayo.edu (Z.-Z.Y.), ansell.stephen@mayo.edu (S.M.A.).

AUTHOR CONTRIBUTIONS

Z.-Z.Y. and S.M.A. designed the research, analyzed data, and wrote the paper; Z.-Z.Y., H.J.K., H.W., and T.P.-T. performed experiments and analyzed data; J.C.V. and S.J. analyzed data and wrote the paper; R.A.L. and A.J.N. wrote the paper; and M.-Y.C.P. analyzed data. All authors approved the final manuscript.

SUPPLEMENTAL INFORMATION

Supplemental Information can be found with this article online at https://doi.org/10.1016/j.celrep.2019.01.085.

DECLARATION OF INTERESTS

The authors declare no competing interests.

Graphical Abstract

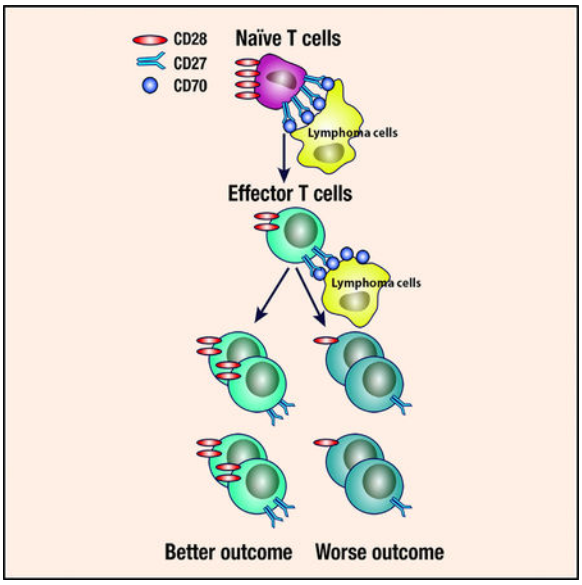

INTRODUCTION

The tumor microenvironment plays a critical role in the regulation of antitumor immunity, thereby impacting patient outcome in follicular lymphoma (Alvaro et al., 2006; Dave et al., 2004; Glas et al., 2007). Previous studies have identified T cell subsets with distinctive functional properties, such as T_H1, T_H2, T_H17, T_H22, and T_{reg} (Duhen et al., 2009; Harrington et al., 2005; Nograles et al., 2009; Park et al., 2005). In addition to these canonical T cell subsets, specific T cell subsets have recently been shown to play crucial roles in immunogenic dysregulation characteristic of certain disease states, such as cancer. For example, in B cell non-Hodgkin lymphoma, our group has identified involvement of TIM-3^+ (Yang et al., 2012) and LAG-3^+ (Yang et al., 2017) T cells in cytokine-induced T cell exhaustion and have demonstrated a role for $CD70^+$ T cells in transforming growth factor β (TGF-β)-mediated T cell inhibition (Yang et al., 2014) within the tumor microenvironment.

Follicular lymphoma (FL) is an indolent B cell malignancy characterized by an extensive but poorly functional T cell infiltrate in the tumor microenvironment. Chemoimmunotherapy is effective in treating FL and rituximab, an anti-CD20 antibody (Ab), combined with chemotherapy (including bendamustine or CHOP) has significantly improved outcomes for FL patients. However, although the median 5-year overall survival reached 74% in FL patients treated with chemoimmunotherapy, a subset of patients who progress early have a very poor outcome (Maurer et al., 2016). Previous studies have found that an impaired immune response to malignant lymphoma cells accounts in part for the poor outcome in this subset of patients (Dave et al., 2004).

In FL, increased numbers of intratumoral T cells overall is an immune signature that correlates with the favorable outcome (Dave et al., 2004; Wahlin et al., 2007). However, the

prognostic significance of intratumoral T cells is controversial in that T cell subsets may either positively or negatively correlate with patient outcome (Laurent et al., 2011; Lee et al., 2006; Wahlin et al., 2010). The prognostic impact of T cells overall may also be influenced by the treatment given. Therefore, the question arises whether a specific T cell signature predominantly predicts patient outcome in FL. In FL, the canonical T cell subsets only account for a portion of intratumoral T cells, and the phenotype of many intratumoral T cells is not well described. In addition, the effect of malignant cells on functional characteristics of known T cell subsets, such as exhausted T cells, T helper cells, and senescent T cells, has not been extensively studied, in part due to limitations in traditional methodologies.

The emergence of mass cytometry or CyTOF (cytometry by time of flight) has revolutionized single-cell proteomics, enabling a comprehensive understanding of cell phenotype, signaling pathways, and function (Amir et al., 2013; Bendall et al., 2011; Wang et al., 2012). CyTOF offers tremendous advantages over the conventional flow cytometer by providing 135 detection channels and the ability to measure more than 40 markers per cell.

CyTOF has been used to characterize the B cell infiltrate in FL patients (Wogsland et al., 2017), but the T cell subsets in FL have not been comprehensively defined. In the present study, we employed CyTOF with a broad range of surface markers to characterize intratumoral T cells from a cohort of FL specimens and from non-malignant tissues that served as controls. We extracted clinical data from the FL patients and used CyTOF to determine which T cell subsets were associated with patient outcome in FL. Our data provided a global picture of intratumoral T cell diversity in FL but also identified subpopulations of intratu-moral T cells that lack CD27 and CD28 expression in part due to the presence of lymphoma B cells. These findings have therapeutic potential for FL patients in that inhibitory and suppressed T cell subsets lacking co-stimulatory receptors could be specifically activated.

RESULTS

The Overall T Cell Profile in FL Patients Differs from Normal Controls

To profile T cells within the FL microenvironment, we performed CyTOF on viably cryopreserved single-cell suspensions from 31 newly diagnosed FL tumors and non-malignant control tissues from healthy individuals, including 3 reactive lymph nodes (rLN), 4 reactive spleens (rSP), and 6 tonsils. Our CyTOF staining panel included a broad range of phenotypic markers that allowed segregation of previously described T cell subsets (Table S1).

We first evaluated whether the FL microenvironment displayed a distinct T cell profile compared to control tissues on a global level. For this, we performed t-distribution stochastic neighbor embedding (tSNE) analysis to characterize the cellular profile in the tumor microenvironment and control tissues. We used increasing numbers of surface makers (see STAR Methods) and utilized tSNE to analyze cell subsets in FL, rLN, rSP, and tonsil specimens. To minimize the variance between samples, we concatenated all files of $CD3^+$, $CD4^+$, or $CD8^+$ cells from each FL, rLN, rSP, or tonsil sample into a single representative file. As the numbers of clustering parameters added to the analysis increased, overall

visualization of tSNE map for $CD3^+$, $CD4^+$, and $CD8^+$ subsets in FL exhibited increasing differences between FL and control tissues (rLN, rSP, and tonsil; Figure 1A). Supporting this, a principal-component analysis (PCA) showed that, although they were more diffusely spread in control tissue (rLN, rSP, and tonsil), the coordinates were more clustered in FL specimens (Figure 1B). Taken together, this global multi-parameter analysis suggested that the T cell population in FL tumors exhibited a distinct T cell profile when compared to control tissues.

Within these global profiles, we observed that the expression of typical surface markers differed between intratumoral T cells in FL and controls (rLN, rSP, and tonsil; Figures S1–S3). Specifically, the numbers of naive T cells ($CD45RO^-CCR7^+$; T_N) were significantly lower in FL than tonsil (Figure 1C), suggesting that T cells from FL were more likely to have a memory phenotype. Perhaps as a result of persistent and chronic antigenic stimula tion present in tumor microenvironment, the population of terminally differentiated cells ($CD45RO^-CCR7^-$; T_{EMRA}) was enriched in FL (Figure 1C).

Multiple T Cell Subsets Are Present in Tumor Microenvironment of FL

To better characterize the phenotype of $CD4^+$ cells in FL and to determine whether they constitute canonical or novel T cell subsets, we performed a tSNE analysis (Simoni et al., 2017). As shown in Figure 2A, we identified 12 distinct cell subsets (S1–S12) in $CD4^+$ T cells from FL and tonsils based on the phenotypic similarity. Overall, $CD4^+$ cells from S1–S7 displayed a phenotype of effector memory type, and cells from S8–S12 were either naive or central memory or terminally differentiated memory type (Figure 2B). The frequency of each memory type subset varied among the patients as indicated by a broad SD. Compared to tonsil tissues, however, cell numbers from S1, S4, S8, and S12 were significantly higher in FL, suggesting increased numbers of T_{reg} cells, exhausted T cells, anergic effector memory T cells, and terminally differentiated T cells in FL. In contrast, cell numbers from S6, S9, and S11 were higher in tonsil than FL (Figure 2C), indicating that activated effector memory cells and naive T cells were highly represented in tonsil tissue. Notably, cell subsets S4, S8, and S12 were almost negligible in tonsil tissue but quite prevalent in FL, suggesting an expansion of terminally differentiated T cells in the lymphoma microenvironment.

Among effector memory cells, both S1 and S2 were $CD25^+$ T cells; however, S2 expressed PD-1 and cells from S1 lacked PD-1 expression. In contrast, cells from S3–S6 were $PD\text{-}1^+$ cells but were $CD25^-$. The $CD45RO^+$ cells (memory) comprised these subsets (S1–S6) as well as S7 and S11 subsets. S7 and S11 differed by expression of co-stimulatory molecules CD27/CD28 as well as CD127, which were expressed on cells from S11, but not S7. Cells from both S8 and S12 were $CD45RO^-CCR7^+$, suggesting a terminally differentiated memory cell type. Of these, S8 expressed T cell markers, such as CD5, CD7, and CD11a and CD127, although cells from S12 were negative for those markers.

In addition to the predominately memory type subsets (such as T_{reg} cells and T_{FH} cells) present in FL, $CD4^+$ naive T cells were variably present in FL biopsy specimens and could be grouped into two subsets (S9 and S10) based on phenotype ($CD45RO^-CCR7^+$; Figure 2D). Although the S9 population displayed a typical phenotype of naive T cells, S10 lacked CD127 and CD44 expression and showed weak expression of a number of markers, such as

CD7, CD5, CD27, and CD28, suggesting a distinct naive population from a conventional naive cell population (S9; Figure 2E).

Next, we tested whether any of the cell populations were associated with patient outcome and found that naive $CD4^+$ T cells were associated with a favorable survival outcome in FL. Patients who had more S9 cells in the $CD4^+$ population survived longer than patients who had less S9 cells (Figure 2F). Similarly, patients who had increased S10 cells in $CD4^+$ population survived longer than patients who had decreased S10 cell, although this did not achieve statistical significance (Figure 2F). We found it somewhat surprising that naive (S9 and S10) rather than memory cells were associated with a favorable prognosis and looked for cell populations that may have a negative impact on prognosis. We noted that multiple populations of $CD4^+CD45RO^+$ cells were positive for CD25 or PD-1 expression (Figure 2B), suggesting that T_{reg} cells or exhausted T cell populations could account for the fact that memory cells were not associated with a favorable prognosis.

PD-1 Expression Distinguishes Activated T Cells from Intratumoral $CD4^+CD25^+$ T_{reg} Cells

We next sought to characterize $CD4^+CD25^+$ T cells (commonly assumed to be T_{reg} cells) in FL, as it has been documented that $CD4^+CD25^+$ T cells are elevated in FL (Hilchey et al., 2011; Yang et al., 2006). Using our CyTOF panel, we confirmed enrichment of $CD4^+CD25^+$ T cells in this cohort (Figure 3A; $p = 0.0395$) and further characterized the phenotype of intratumoral $CD4^+CD25^+$ T cells compared to $CD4^+CD25^-$ T cells. Both tSNE and cluster analysis showed a distinct profile between $CD4^+CD25^-$ and $CD4^+CD25^+$ T cells from biopsy specimens of FL (Figures S4A and S4B). The $CD4^+CD25^+$ population was more likely to contain memory cells than the $CD4^+CD25^-$ population because the vast majority of $CD4^+CD25^+$ T cells were $CD45RO^+$. As expected, CD127 and CCR4 were reciprocally expressed on $CD4^+CD25^-$ and $CD4^+CD25^+$ T cells. $CD4^+CD25^+$ T cells tended to express low levels of PD-1 ($PD\text{-}1^{low}$) and lack CXCR5 expression, suggesting an extrafollicular location, as high levels of PD-1 ($PD\text{-}1^{high}$) and CXCR5 are exclusively expressed on T cells in follicles in FL (Figures S4C and S4D). Interestingly, $CD4^+CD25^+$ T cells displayed higher expression of activation-related molecules, including CD27, CD28, and CD69, suggesting an activation phenotype for $CD4^+CD25^+$ T cells (Figure S4D).

It is unknown whether $CD4^+CD25^+$ T cells display a similar phenotype between FL and tonsil given that these two entities have distinct microenvironments. To evaluate the potential differences, we concatenated data from the 31 FL patient samples into 1 file and data from the 6 tonsils into a second file and ran a tSNE analysis on the $CD4^+CD25^+$ T cells. As shown in Figure 3B, the tSNE maps of $CD4^+CD25^+$ T cells were quite different between FL and tonsil. Specifically, we observed that $CD4^+CD25^+$ T cells in FL exhibited decreased expression level of CD28, CD27, CD69, and PD-1 as well as CD5 and CD7 when compared to tonsil specimens (Figure 3C). As a result of increased $CD4^+CD25^+$ T cells in FL that express T cell immunoreceptor with Ig and ITIM domains (TIGIT) (Figure S4E), TIGIT expression was greater in FL specimens than in tonsil tissue. The finding that many $CD4^+CD25^+$ T cells had differing expression of activation markers or expression of receptors, such as TIGIT and PD-1, suggested that $CD4^+CD25^+$ T cells may not be a single

population but that some may represent a population of T_{reg} cells with an activated phenotype.

To validate the presence of two $CD4^+CD25^+$ subsets in the FL microenvironment, we used tSNE to interrogate the $CD4^+CD25^+$ population in representative FL samples. Indeed, this analysis confirmed two subsets (S1 and S2) of intratu-moral T cells that express CD25 (Figure 3D). PD-1, expressed predominantly in the S2 subtype, was a major segregator of S1 ($CD4^+CD25^+PD\text{-}1^-$) and S2 ($CD4^+CD25^+PD\text{-}1^+$) subsets, both of which expressed CCR4 (Figure 3D). Additionally, S1 tended to express reduced levels of activation markers CD27, CD28, CD69, and TIGIT compared to S2 (Figure 3E), indicating that S2 has an activated phenotype when compared to S1. Furthermore, the S2 subset had higher levels of CD45RO expression and lower expression of CCR7 than the S1 subset, consistent with a memory phenotype due to activation (Figure 3E). Cells from S1 and S2 in tonsil tissues exhibited a similar phenotype to those from FL (Figure S4F). We found that S2 was more prevalent than S1 in tonsil specimens although the numbers of S1 cells were significantly higher than S2 cells in FL ($p < 0.0001$; Figure 3F). Taken together, these results suggest that $CD25^+$ T_{reg} cells are heterogeneous and PD-1 expression defines two subsets of T_{reg} cells with distinct phenotype in FL.

PD-1-Expressing T Cells Are Heterogeneous, and Subsets of PD-1^+ T Cells Are Associated with Overall Survival in FL

Predicated on our previous studies demonstrating heterogeneity within PD-1^+ cells of the lymphoma microenvironment (Yang et al., 2012, 2015, 2017), we next focused on characterizing PD-1^+ T cell phenotypes within FL using our CyTOF panel. In this cohort, approximately 71.5% of intratumoral $CD3^+$ T cells expressed PD-1 with either low or high intensity (Figure S1). Among these T cells, $CD4^+$ T cells expressed high levels of PD-1 and $CD8^+$ T cells expressed relatively lower levels of PD-1, which was confirmed by CyTOF shown in both two-dimension plots and tSNE maps (Figures 4A and 4B). Within intratumoral $CD4^+$ T cells, 26.8% and 44.3% were PD-1^{high} and PD-1^{low}, respectively (Figure 4C). Conversely, $CD8^+$ T cells lacked a $PD1^{high}$ population and were PD-1^{low} in 67.9% of cells (Figure 4C).

Using tSNE analysis, we were able to identify 4 subsets (S3–S6) of $CD4^+CD25^-$ T cells that express PD-1 in FL (Figure 4D). Consistent with our previous finding (Yang et al., 2015), a subset of PD-1^+ T cells could be segregated by CXCR5 expression and defined the population of follicular T helper (T_{FH}) cells (S3). Cells from both S4 and S5 displayed reduced expression of co-stimulatory molecules CD27 and CD28, and cells from S3 and S6 were positive for expression of these receptors. CCR4 expression, however, was useful in segregating S4 and S5, as we found that CCR4 was expressed on cells from S5 but expression was negligible on cells from S4 (Figure 4D). Cells from S4 and S5 exhibited reduced levels of CD45RO, CD69, CD5, and TIGIT when compared to those from S3 and S6 (Figure 4E). These results suggest that cells from S6 may represent a population of activated cells, and cells from S4 appeared to be exhausted cells. Despite these different subsets, tSNE maps revealed that the phenotypes of subsets S3 and S6 or S4 and S5, respectively, were relatively similar. As shown in Figure 4F, S3 ($CXCR5^+$) and S6

(CXCR5$^-$) showed an overall similar tSNE structure and a similar expression pattern of a number of surface markers, including CD27 and CD28, although CXCR5 expression distinguished the 2 subsets from each other. In contrast, although S4 (CCR4$^-$) and S5 (CCR4$^+$) displayed an overall similar tSNE structure, these two subsets had a tSNE structure markedly different from subsets S3 and S6. As expected, distribution pattern of surface markers, such as CD27 and CD28, in S4 and S5 was different from S3 and S6. We then utilized flow cytometry to determine whether there was loss of CD27 or CD28 expression on PD-1$^+$ T cells in FL biopsy specimens. As shown in Figure S5A, we could detect CD27$^-$, CD28$^-$, or CD27$^-$CD28$^-$ subpopulations in the PD-1$^+$ T cell population, although the frequency of these subsets was lower when compared to the frequency in the PD-1$^-$ T cell population.

Interestingly, although the total PD-1$^+$ T cell expression level did not predict patient outcome in FL, we observed that subsets of PD-1$^+$ T cells were associated with overall survival. As shown in Figure 4G, higher frequency of S3 and S6 populations (characterized by activation phenotypes) correlated with a better overall survival. In contrast, higher frequency of S4 and S5 populations (characterized by reduced expression of co-stimulatory molecules and activation markers) were associated with an inferior overall survival in FL, although the difference is not statistically significant for the S4 subset (Figure 4G). There was no statistically significant correlation between any of the T cell subtypes and the histologic grade of FL. An association with transformation to large-cell lymphoma could not be shown as too few patients transformed (n = 2). These results indicate that phenotypes of intratumoral T cells with altered expression of co-stimulatory molecules and activation markers may play a role in patient outcome in FL.

T Cells Deficient in Co-stimulatory Molecules Are Prevalent in FL and Predict Patient Outcome

Because co-stimulatory molecules play a crucial role in T cell activation and function, we surmised that loss of CD28 and CD27 in subsets of memory cells (S1, S3, and S4) was responsible for the lack of association between the abundance of memory T cells and favorable clinical outcome. To define the expression of CD27 and CD28 in FL and tonsil, we generated a tSNE map using the combined samples (Figure 5A). Indeed, the number of CD27$^-$, CD28$^-$, or CD27$^-$CD28$^-$ T cells was significantly higher in FL than tonsil (Figure 5B). We further confirmed the loss of CD27 on intratumoral T cells in FL by flow cytometry and immunohistochemistry (Figures S5B and S5C).

We then examined which T cell populations were more susceptible to the loss of co-stimulatory molecules. Deficiency of CD28 or CD27 was distributed across the tSNE map, suggesting that loss of these co-stimulatory molecules occurred in a variety of T cell populations. Specifically, CD25$^-$ T cells had an increased percentage of CD27$^-$ or CD28$^-$ cells relative to CD25$^+$ T cells. We also observed that PD-1$^-$ (PD-1^{neg}) T cells tended to lose CD27 or CD28 expression when compared to PD-1$^+$ (PD-1^{high} plus PD-1^{low}) T cells. In terms of cell differentiation, terminally differentiated T cells (T_{EMRA}) displayed greater loss of these co-stimulatory molecules than other non-T_{EMRA} cells (Figure 5C).

The lack of CD27 or CD28 on T cells was also associated with the lack of other markers. As shown in Figure 5D, T cells deficient in CD27 or CD28 exhibited decreased expression of CD5 and CD7. $CD27^-$ or $CD28^-$ T cells also had reduced expression of activation markers, including CD25, CD69, and TIGIT (Figure 5D). These results suggest that $CD27^-$ or $CD28^-$ T cells are likely anergic or senescent T cells.

We then determined whether CD27 and CD28 loss was associated with patient survival. Using the Kaplan-Meier method, we found that the loss of CD27 expression was significantly associated with an inferior overall survival in FL patients ($p = 0.0073$). The loss of CD28 expression showed a similar trend but did not reach statistical significance in this cohort. Similarly, the number of intratumoral $CD3^+$ T cells lacking both CD27 and CD28 expression was associated with a significantly poorer survival ($p = 0.012$; Figure 5E). We observed that CD27 loss was a key prognostic factor to further stratify patients by overall survival in conjunction with other markers. As shown in Figure 5F, although $CD25^+$ or PD-1^+ T cells alone failed to predict patient outcome, when stratified by CD27 expression, both $CD25^+$ and PD-1^+ T cells showed a significant correlation with overall survival in FL.

Loss of Co-stimulatory Receptor Expression Represents a Distinct Immune Signature in FL

We next explored whether immune signatures could be identified within the FL cohort using a clustering approach. To do this, we used single-marker frequency from $CD3^+$ T cells from all FL intratumoral specimens and performed clustering analysis using the software Cluster 3.0. As shown in Figure 6A, two main clusters were identified, and these could be distinguished in part by the presence or absence of CD27, CD28, CD5, and CD7 co-expression.

To explore whether this clustering had clinical relevance, we then ran the analysis using the software CITRUS to identify significant clusters between patients alive or dead with long-term follow-up (Figure 6B). Using a CITRUS analysis setting that included the minimum cluster size of 5% and false discovery rate (FDR) of 1%, we identified 10 clusters that differed between patients alive and patients who died (Figure 6B). We divided these 10 clusters into 4 parent clusters (21536, 21534, 21539, and 21532) according to a unique feature of redundant events. The clusters derived from $CD4^+$ T subsets were defined by distinct phenotypes (Figure S6A): cluster 21536, T_{EMRA} cells ($CD45RO^+CCR7^-CD127^-$); cluster 21539, T_N cells ($CD45RO^{low/-}CCR7^+CD127^+$); cluster 21534, T_H1 cells ($CXCR3^+$); and cluster 21532, T_{FH} cells ($CXCR5^+$PD-1^+; Figures 6C and S6B). Each cluster was confirmed to have a unique phenotype. For example, cluster 21536 had reduced levels of CD27, CD28, CD7, CD11a, and CD69 and cells from other clusters had expression of these T cell markers. The abundance of clusters 21536 and 21534 was lower in live patients than deceased patients, although the opposite result was seen for clusters 21539 and 21532 (Figures 6C and S6C).

Given the unique phenotype of these clusters, we wondered whether any of these clusters had prognostic impact in FL. By extracting the abundance events of these 10 clusters from each patient of this cohort, we analyzed survival curve using the Kaplan-Meier method. Although most of these clusters failed to predict patient survival, clusters 21536 and 21523

showed that lower expression of these markers (Figure S6C) may be associated with better overall survival (Figure 6D). Given that clusters 21536 and 21523 displayed a phenotype of reduced expression levels of CD27, CD28, CD7, CD11a, and CD69, this result was consistent with the finding that the loss of CD27 expression was significantly associated with inferior overall survival in FL patients (Figure 5F). This result was also consistent with the finding by the Cluster 3.0 analysis that loss of expression of CD27, CD28, CD5, and CD7 was one of the major clusters in FL (Figure 6A). In this cohort, expression of CD27, CD69, and TIGIT were found to be associated with patient outcome. However, the capacity of CD27 loss to further stratify patients by overall survival was extended to almost all the markers used for CyTOF staining panel (Table S3). In contrast, CD69 or TIGIT failed to further stratify patients when combined with most markers (Table S3). Taken together, these results suggest that unique immune signatures stratifying patients by outcome are present in FL and that CD27 loss has a dominant role in predicting patient outcome.

$CD70^+$ Lymphoma Cells Induce Downregulation of CD27 or CD28 Expression on Intratumoral T Cells, which Impairs Their Capacity to Proliferate

Given our finding of $CD27^-$ and $CD28^-$ T cell enrichment in the FL microenvironment and its association with clinical outcome, we explored the underlying mechanism that accounts for loss of CD27 and CD28. We sorted intratumoral $CD3^+$ T cells by flow cytometry into $CD27^+CD28^+$ T cells or cells that lack expression of either CD27 or CD28 or both (Figure S7A). We first determined whether intratumoral T cells were prone to lose CD27 or CD28 expression by activation through TCR stimulation. As shown in Figure 7A, expression of CD27 or CD28 was downregulated in a time-dependent manner when T cells were cultured in anti-CD3-coated plate plus anti-CD28 Ab and compared to cells cultured in uncoated normal plate. In addition to activation, stimulation with cytokines, including TGF-β, also reduced expression of CD27 or CD28 on T cells (Figure 7B). Both activation- and TGF-β-induced downregulation of CD27 or CD28 expression was associated with upregulation of CD70 on T cells (Figures S7B and S7C).

In FL, CD70 was abundantly expressed on malignant lymphoma B cells when compared to tonsil tissue (Figure 7C) when assessed by immunohistochemistry, and this was confirmed by flow cytometry (Figure 7D). We then wanted to test whether CD70-expressing lymphoma cells play a role in the regulation of CD27 or CD28 expression on intratumoral T cells. We used the transformed FL cell line—DoHH2—that expresses high levels of CD70 on the cell surface (Figure 7Ei) and co-cultured the cell line with T cells in anti-CD3 Ab-coated plates with anti-CD28 Ab for 3 days. To minimize the effect of DoHH2 cell proliferation on T cell activation, we pretreated DoHH2 cells with actinomycin D to arrest the cell cycle, thereby blocking cell growth. As shown in Figure 7Eii, expression of both CD27 and CD28 was downregulated on T cells co-cultured with DoHH2 cells. Next, we pretreated DoHH2 cells with an anti-CD70 Ab and determined whether blocking CD70 expression on DoHH2 cells reversed the downregulation of CD27 expression. When incubated with an anti-CD70 Ab, less CD70 was detected on DoHH2 cells (Figure 7Eiii). We found that downregulation of CD27 expression on T cells co-cultured with anti-CD70 Ab-pre-incubated DoHH2 cells was reversed when compared to T cells co-cultured with immunoglobulin G (IgG)-preincubated DoHH2 cells (Figure 7Eiv), a finding that could not be replicated when T cells were co-

cultured with normal B cells that lacked CD70 expression (data not shown). Other $CD70^+$ B cell lines, including Raji (Burkitt's lymphoma) and Mec-1 (chronic B cell leukemia) cells, showed a similar effect. T cells co-cultured with Mec-1 or Raji cells also displayed reduced expression of CD27 and CD28 (Figures S7D and S7E). These results suggest that CD70-expressing lymphoma B cells are involved in CD27 down-regulation seen in FL.

Finally, we wanted to test whether loss of CD27 or CD28 impacted T cell proliferation. To test this, we flow sorted $CD27^-CD28^+$, $CD27^+CD28^-$, $CD27^-CD28^-$, or $CD27^+CD28^+$ T cells from lymphoma tissue and labeled these cells with carboxyfluorescein succinimidyl ester (CFSE) to monitor cell proliferation. Cells were cultured in an anti-CD3-coated plate in the presence of anti-CD28 Ab for 3 days and harvested for flow cytometry analysis. As shown in Figure 7F, $CD27^+CD28^+$ T cells showed the greatest capacity for proliferation among the T cell subsets as a median of 85.1% of cells were $CFSE^{dim}$ (proliferated) cells. Compared to $CD27^+CD28^+$ cells, $CD27^+CD28^-$, $CD27^-CD28^-$, or $CD27^-CD28^+$ T cells either lost ability to proliferate or displayed significantly reduced cell proliferation as indicated by a decreased number of $CFSE^{dim}$ cells. The findings are consistent with the observation that $CD27^-$ or $CD28^-$ T cells were highly represented in the terminally differentiated cell population (Figures 5C and 7G). These results suggest that, although CD28 expression is crucial, CD27 expression also plays an important role in T cell activation and proliferation. Cells lacking expression of CD27 and CD28 are therefore poorly functional, and increased numbers of these cells in FL limit an effective anti-tumor immune response.

DISCUSSION

Using conventional flow cytometry and immunohistochemistry, subsets of T cells in the tumor microenvironment of FL have been quantitatively and qualitatively defined (Yang et al., 2006, 2009, 2012, 2014, 2015). In the present study, we sought to more comprehensively define T cell phenotypes in FL using a CyTOF panel of 33 markers to interrogate phenotypes within biopsy specimens from a cohort of 31 FL patients and control tissues. This approach identified T cell populations within the FL microenvironment with prognostic significance in this cohort. Most importantly, we showed that co-stimulatory receptors, CD27 and CD28, are frequently lost on T cell subsets in FL, providing additional evidence to support previous findings describing a suppressive tumor microenvironment in FL (Hilchey et al., 2011; Yang et al., 2012). Importantly, we showed that loss of these receptors was associated with poor outcome and may be caused in part by CD70 expression on tumor cells.

Global analysis identified differences between the FL tumor immune microenvironment and normal activated tissue visualized by both tSNE and PCA analysis. The tSNE map revealed that intratumoral T cells in FL are heterogeneous, which is consistent with previous studies (Amé-Thomas et al., 2012; Wahlin et al., 2010). Combined with tSNE analysis, we identified at least 12 subsets from intratumoral $CD4^+$ T cells with 3 subsets that are clearly present in FL and are virtually absent from control tissue. These 3 subsets include exhausted effector memory cells and terminally differentiated T cells. This subset identification

represents a way to explore the heterogeneity of intratumoral $CD4^+$ T cells in FL that traditional flow cytometry may not achieve.

Studies have shown that not all $CD4^+CD25^+$ T cells are T_{reg} cells and some are simply activated T cells. Our data showed that PD-1 expression defined a T_{reg} subset of $CD4^+$ $CD25^+$ (S2) as activation-like T cells. Supporting this, we found that this subset expressed increased levels of co-stimulatory and activation markers CD27, CD28, and CD69 when compared to other $CD4^+CD25^+$ T cells. Consistent with previous studies, we found that T_{reg} cells expressed high levels of PD-1 (Tang et al., 2004) and PD-1 expression discriminated T_{reg} cells from activated T cells (Raimondi et al., 2006).

PD-1 is expressed on a large portion of intratumoral T cells, and $PD\text{-}1^+$ cells account for approximately 70% of intratumoral T cells in FL (Yang et al., 2015). Given such high frequency, more diversity and heterogeneity of PD-1-expressing T cells is anticipated. By CyTOF, we could clearly identify T_{FH} cells that expressed PD-1 but also found that the remaining $PD\text{-}1^+$ T cells could be further divided into different subsets using CCR4, CD27, and CD28 expression. One subset of $PD\text{-}1^+$ T cells expressing CD27 and CD28 (S6) had high expression of CD69 and other activation-related markers, suggesting an activated phenotype of this population, given that PD-1 itself is also an activation marker. A second subset (S5) was $CD25^-$ but expressed CCR4. Our previous studies had shown that intratumoral T_{reg} cells express CCR4 (Yang et al., 2006) and can be $CD25^-$ (Yang et al., 2007), and therefore, $CD4^+CCR4^+PD\text{-}1^+$ T cells (S5) likely represent a subset of atypical T_{reg} cells. This segregation is especially meaningful when PD-1 expression is used to predict patient survival. The correlation between intratumoral $PD\text{-}1^+$ T cells and patient outcome in FL has been controversial, with some studies finding that PD-1 expression correlates with a superior outcome and other studies showing an association with an inferior outcome in FL (Carreras et al., 2009; Muenst et al., 2010; Richendollar et al., 2011). This study shows that, when the total number $PD\text{-}1^+$ T cells are analyzed, PD-1 expression is not significantly associated with patient outcome. However, when $PD\text{-}1^+$ subsets are identified, patients with more S4 and S5 subsets are associated with a poor survival in FL, and patients with more S3 and S6 subsets correlate with a better outcome.

Our data show that loss of co-stimulatory molecules expression is a dominant immune signature that correlates with poor survival in FL. Although loss of co-stimulatory receptors on T cells may be seen in elderly people (Effros, 1997; Vallejo et al., 1998) and patients with autoimmune diseases, such as rheumatoid arthritis (Lee et al., 2007; Schmidt et al., 1996; Żabińska et al., 2016), we observed that intratumoral T cells deficient of CD27 and CD28 expression were highly represented in FL. These T cells also tend to lose expression of CD5 and CD7, consistent with previous data (Schmidt et al., 1996). Previous studies have shown that interaction with CD70 results in downregulation of CD27 expression on T cells (Hintzen et al., 1994), and we find that $CD70^+$ lymphoma cells contribute to the generation of $CD27^{low}$ cells in patients with FL.

Given important roles of these surface markers for T cells, we anticipated that T cell function would be impaired by their loss. Indeed, we found that, phenotypically, $CD27^-$ or $CD28^-$ T cells showed reduced expression of other activation-related markers, and

functionally, these T cells displayed decreased proliferation in response to TCR stimulation. As a result, we observed that increased numbers of $CD27^{-}CD28^{-}$ T cells in the tumor micro-environment correlated with a worse clinical outcome in FL. This observation is in line with the finding that CD27 is required for generation and long-term maintenance of T cell immunity (Hendriks et al., 2000). Importantly, we identified several clusters that differed between patients who were still alive with ongoing follow-up and patients who had died. One of these clusters, with a $CD27^{-}CD28^{-}CD7^{-}CD69^{-}$ phenotype, predicted patient outcome in FL. This further confirmed the finding that loss of CD27 expression is associated with a poor outcome in FL.

Although these findings are exploratory in nature, they are of particular relevance in the era of immune checkpoint therapy when agents, such as anti-PD-1 antibodies, are being tested in clinical trials for many diseases, including FL. Our data confirm the expression of PD-1 on many intratumoral T cell subsets but also find that some of these subsets lack expression of CD28 and CD27. Recent data have shown that the co-receptor CD28 is strongly preferred over the T cell receptor (TCR) as a target for dephosphorylation by PD-1-recruited Shp2 phosphatase (Hui et al., 2017). It was further shown that CD28, and not the TCR, is preferentially dephosphorylated in response to PD-1 activation by PD-L1 in an intact cell system, suggesting that PD-1 suppresses T cell function primarily by inactivating CD28 signaling. Increased populations of $PD\text{-}1^{+}CD28^{-}CD27^{-}$ intratumoral T cells in FL, as found in this study, may explain the modest clinical benefit from treatment with the PD-1 blocking antibodies nivolumab and pembrolizumab in this patient population (Ding et al., 2017; Lesokhin et al., 2016). Although it was expected that increased PD-1 expression in FL would result in high response rates to PD-1 blockade, response rates have been low and responses have not been durable. The loss of co-stimulatory receptors on the PD-1-positive cells likely explains the lack of clinical benefit, and the prevalence of cells lacking costimulatory receptors may be a biomarker for response in FL.

Of note, however, the prognostic value of the biomarkers presented in this work should be tempered with the recognition of some limitations of the data. First, due to the exploratory nature of the study, we did not perform an adjustment for multiple comparisons. Second, because of the small sample size and our inability to adjust for some of the known prognostic variables, including the Follicular Lymphoma International Prognostic Index (due to missing data) in this patient series, it is possible that the observed association between the biomarkers under study and patient survival may be confounded by other clinicopathologic variables that were not adjusted for in an univariate analysis. As such, any prognostic findings will need to be further validated in other independent patient cohorts.

In summary, using CyTOF, we identified subsets of T cells that are present in FL but virtually absent in tonsil. Furthermore, we found that $CD4^{+}PD\text{-}1^{+}$ T cells are heterogeneous and some subsets correlate with FL patient survival. Notably, we identified that the loss of co-stimulatory receptors, including CD27 and CD28, defines an immune signature that correlates with patient outcomes in FL, and this signature is driven in part by CD70 expression on the malignant cells. Taken together, these results provide important information to further understand the tumor microenvironment in FL and potential benefit from immunological therapies.

STAR★METHODS

CONTACT FOR REAGENT AND RESOURCE SHARING

Further information and requests for resources and reagents should be directed to and will be fulfilled by the Lead Contact, Zhi-Zhang Yang (yang.zhizhang@mayo.edu).

EXPERIMENTAL MODEL AND SUBJECT DETAILS

Patient Samples—Patients providing written informed consent were eligible for this study if they had a tissue biopsy that on pathologic review showed follicular B cell non-Hodgkin lymphoma (NHL) and adequate tissue to perform the experiments. The patients were seen at our hospital from November 1984 to November 2009. The use of human tissue samples for this study was approved by the Institutional Review Board of the Mayo Clinic/Mayo Foundation. Patient characteristics, including age, sex, and health status, are summarized in Table S2. Lymph nodes, tonsils and spleen tissue from adult patients without lymphoma served as controls.

Mononuclear cells were isolated from biopsy specimens of patients or healthy donors using centrifugation over Ficoll Paque solution. T cell subsets were isolated by either microbeads or flow sorter and subjected to primary culture for assays. For functional assays, T cells were cultured in OKT-coated plates with anti-CD28 Ab in RPMI 1640 medium containing 10% fetal bovine serum, 1% penicillin-streptomycin (10,000 U/mL and 10,000 μg/mL, respectively) in an incubator containing 5% CO_2 at 37°C.

Cell lines—Three cell lines (DoHH2, Raji and Mec-1) were used in the study. DoHH2 cell line was established from the pleural effusion of a 60-year-old man with refractory immunoblastic B cell lymphoma progressed from follicular centroblastic/centrocytic lymphoma. Raji cell line was established from 11-year-old boy with Burkitt's lymphoma. Mec-1 cell line was established from the peripheral blood of a 61-year-old Caucasian man with chronic B cell leukemia. These cells were cultured in RPMI 1640 medium containing 10% fetal bovine serum, 1% penicillin-streptomycin (10,000 U/mL and 10,000 μg/mL, respectively) in an incubator containing 5% CO_2 at 37°C. Culture medium was changed by centrifugation (300 × g for 5 minutes) with subsequent resuspension of the cell pellet in fresh medium.

METHOD DETAILS

Cell isolation and purification—Fresh tissue biopsy specimens from FL tumors, reactive lymph nodes, reactive spleens and tonsils were gently minced over a wire mesh screen to obtain a cell suspension. The cell suspension or peripheral blood from patients or healthy donors was centrifuged over Ficoll Paque at 500 × g for 15 minutes to isolate mononuclear cells. $CD3^+$ or $CD4^+$ T cells were isolated using positive selection with CD3 or CD4 microbeads kit (StemCell Technologies, Vancouver, Canada). For purification of $CD27^+$, $CD28^+$ or $CD27^+CD28^+$ or $CD27^-CD28^-$ T cells, PBMCs were stained with fluorochrome-conjugated anti-CD3, CD27 and CD28 Abs. After gating on $CD3^+$ T cells, $CD27^+$, $CD28^+$, $CD27^+CD28^+$ or $CD27^-CD28^-$ T cells were isolated by a flow cytometry sorter.

Mass cytometry (CyTOF)—The CyTOF assay was performed according to the manufacturer's instruction. Briefly, 3×10^6 cells were stained with 5 mM Cell-ID™ Cisplatin (Fluidigm, San Francisco, CA) for 5min and quenched with MaxPal Cell Staining Buffer (Fluidigm) using 5 times the volume of the cell suspension. After centrifugation, cell suspensions (50 μl) were incubated with 5 μL of human Fc-receptor Blocking solution (Biolegend, San Diego, CA) for 10min and 50 μL of pre-mixed antibody cocktail (Table S2) for 30 min. After washing, cells were incubated with 1ml of cell intercalation solution (125nM MaxPal Intercalator-Ir into 1ml MaxPal Fix and Pem Buffer, Fluidigm) overnight at 4°C. Cells were centrifuged with MaxPal Water and pelleted. The pelleted cells were suspended with EQ Calibration Beads (Fluidigm) and cell events were acquired by a CyTOF II instrument (Fluidigm).

CyTOF data analysis—The CyTOF data were analyzed using online software Cytobank (Kotecha et al., 2010). All the samples were normalized and analyzed simultaneously to account for variability in signal across long acquisition times. A high-level gating strategy was applied simultaneously to all CyTOF files (Figure S1). For specific analysis purpose, we concatenated all sample files to one file. To generate flow files for certain population, we split files by the population and downloaded them into individual file for each sample. The platforms for tSNE, SPADE and Citrus were used to analyze the data. Linage markers (CD4, CD8, CD25, CD127, PD-1, CXCR5, CCR7 or CD45RO) were usually included in the analysis to distinguish T cells, T_{reg} cells, exhausted cells, naive or memory T cells.

A tSNE map was generated by the t-Distribution Stochastic Neighbor Embedding (tSNE) analysis that makes a pairwise comparison of cellular phenotypes to optimally plot similar cells close to each other and reduces multiple parameters into two dimensions (tSNE1 and tSNE2). For most analysis, we selected equal events for each sample. Channel (markers) selection was variable depending on cell populations to be clustered. We chose the 3,000 iterations, perplexity of 30 and theta of 0.5 as standard tSNE parameters. Specifically, for S1–S12 identification of $CD4^+$ T cells by tSNE analysis, we selected channels of CD25, CCR4, PD-1, CXCR5, CD27, CD28, CCR7, CD127 and TCR-gd to segregate cell populations. After viSNE plots were generated, we first defined $CD25^+$ T subsets based on whether or not PD-1 was expressed (S1–S2). And then, PD-1^+ subsets were segregated from $CD25^-$ T cells based on expression of CXCR5, CCR4, CD27 and CD28 (S3–S6). We defined non-$CD25^+$ and non-PD-1^+ cells as naive or memory cells by expression of CD45RO and CCR7. The memory subsets (CD45RO+CCR7-) were defined using CD5, CD27, CD28 and CD127 (S7, S8). The naive T subsets ($CD45RO^-CCR7^+$) were segregated based on expression of CD127, CD44, CD27 and CD28 (S9, S10). S11 and S2 were defined as central memory ($CD45RO^+CD127^+$) and terminally-differentiated memory ($CD45RO^-CCR7^-$) cells, respectively.

For SPADE analysis, we used 100 target numbers of nodes and 10% downsampled events target. The clustering channels were selected based on whether they were lineage markers and which cell population to be clustered.

For CITRUS (cluster identification, characterization, and regression) analysis, Significance Analysis of Microarrays (SAM) – Correlative and Abundance were selected for Association

Models and Cluster Characterization, respectively. Principal Component analysis was performed to compare the effect of principal components on variables between FL and tonsil specimens. Cluster analysis of intratumoral $CD3^+$ or $CD4^+CD25^-$ or $CD4^+CD25^+$ T cells was performed by Cluster 3.0 to achieve the hierarchical analysis and visualized via the Java TreeView 1.0.5.

Flow cytometry and T cell proliferation—Expression of surface markers on T or B cells was measured by flow cytometry. Cells were washed in phosphate-buffered saline (PBS) and incubated with CD3, CD4, CD8, CD19, PD-1, CD70, CD27 and CD28 specific fluorochrome–conjugated antibodies and analyzed by flow cytometry (Becton Dickinson, San Jose, CA). T cell proliferation was measured using CFSE staining assay. Briefly, cells were washed and resuspended at 1×10^7/mL in PBS. A stock solution of carboxyfluorescein succinimidyl ester (CFSE, 5 mM) was diluted 1:100 with PBS and added to the cells for a final concentration of 5 μM. After 10 minutes at 37°C, cells were washed 3 times with 10 vol PBS containing 10% FBS. CFSE-labeled responding cells were cultured in OKT-coated plate the presence of anti-CD28 Ab at 37°C and 5% CO_2. Cells were harvested at day 3, washed, and stained with fluorochrome-conjugated antibodies for detection of surface markers for 30 minutes at 4°C. Cells were analyzed by flow cytometry. The percentage of $CFSE^{dim}$ were measured and calculated as the percentage of proliferated cells.

Immunohistochemistry—Paraffin embedded tissue was obtained from Mayo Clinic Tissue Registry and the tissue sections were deparaffinized in xylene. After cleared through graded ethanol series, endogenous peroxidase was quenched by incubation in 50% methanol/H_2O_2. The sections were pretreated 30 min with 50 mM EDTA, pH 8.0 using a steamer and cooled for an additional 5 min. The staining was performed automatically on DAKO Autostainerplus using CD70 Ab (LSBio, LS-A8809, 3μg/ml) or mouse IgG1 control (DAKO, #x0931, 1:100000). The sections were stained with hematoxylin and rinsed well in tap water. The slides were observed with light microscopy (Olympus AX70, 200 x/aperture 0.46, 400 x/aperture 0.75, 600 × /aperture 0.80; Olympus America, Melville, NY, USA) with images captured with a SPOT RT camera and software (Diagnostic Instruments, Burlingame, CA, USA).

QUANTIFICATION AND STATISTICAL ANALYSIS

Student’s t test was used to compare the distributions of continuous biomarkers when the normal distribution assumption was adequate. When normal distribution was in question, the non-parametric Wilcoxon rank-sum test was used. For matched-paired data, the paired t test or Wilcoxon sign-rank tests were used. Overall survival was measured from the date of diagnosis until death from any cause. The Kaplan-Meier method was used to estimate overall survival. The univariate associations between individual clinical features and survival were determined with the log-rank test. Due to the exploratory nature of these studies, multiple comparison adjustment was not performed; in all cases, $p < 0.05$ was used to declare statistical significance.

DATA AND SOFTWARE AVAILABILITY

All CyTOF files were deposited at the FlowRepository website (http://flowrepository.org/). The software to analyze these files including viSNE, SPADE and CITRUS were obtained from the Cytobank website (https://cytobank.org/) and need a subscription.

Supplementary Material

Refer to Web version on PubMed Central for supplementary material.

ACKNOWLEDGMENTS

We thank Mr. Sean Murray and Dr. Heather Brown for the technical assistance of use CyTOF II. This work was supported by grants from the NIH (P50 CA97274), the Leukemia & Lymphoma Society (6544-18-01), the Landow Foundation (91314990), the Jaime Erin Follicular Lymphoma Research Consortium (91314125), and the Predolin Foundation (91314099).

REFERENCES

Alvaro T, Lejeune M, Salvadó MT, Lopez C, Jaén J, Bosch R, and Pons LE (2006). Immunohistochemical patterns of reactive microenvironment are associated with clinicobiologic behavior in follicular lymphoma patients. J. Clin. Oncol 24, 5350–5357. [PubMed: 17135637]

Amé-Thomas P, Le Priol J, Yssel H, Caron G, Pangault C, Jean R, Martin N, Marafioti T, Gaulard P, Lamy T, et al. (2012). Characterization of intratumoral follicular helper T cells in follicular lymphoma: role in the survival of malignant B cells. Leukemia 26, 1053–1063. [PubMed: 22015774]

Amir el-A.D., Davis KL, Tadmor MD, Simonds EF, Levine JH, Bendall SC, Shenfeld DK, Krishnaswamy S, Nolan GP, and Pe'er D (2013). viSNE enables visualization of high dimensional single-cell data and reveals phenotypic heterogeneity of leukemia. Nat. Biotechnol 31, 545–552. [PubMed: 23685480]

Bendall SC, Simonds EF, Qiu P, Amir el-A.D., Krutzik PO, Finck R, Bruggner RV, Melamed R, Trejo A, Ornatsky OI, et al. (2011). Single-cell mass cytometry of differential immune and drug responses across a human hematopoietic continuum. Science 332, 687–696. [PubMed: 21551058]

Carreras J, Lopez-Guillermo A, Roncador G, Villamor N, Colomo L, Martinez A, Hamoudi R, Howat WJ, Montserrat E, and Campo E (2009). High numbers of tumor-infiltrating programmed cell death 1-positive regulato ry lymphocytes are associated with improved overall survival in follicular lymphoma. J. Clin. Oncol 27, 1470–1476. [PubMed: 19224853]

Dave SS, Wright G, Tan B, Rosenwald A, Gascoyne RD, Chan WC, Fisher RI, Braziel RM, Rimsza LM, Grogan TM, et al. (2004). Prediction of survival in follicular lymphoma based on molecular features of tumor-infiltrating immune cells. N. Engl. J. Med 351, 2159–2169. [PubMed: 15548776]

Ding W, LaPlant BR, Call TG, Parikh SA, Leis JF, He R, Shanafelt TD, Sinha S, Le-Rademacher J, Feldman AL, et al. (2017). Pembrolizumab in patients with CLL and Richter transformation or with relapsed CLL. Blood 129, 3419–3427. [PubMed: 28424162]

Duhen T, Geiger R, Jarrossay D, Lanzavecchia A, and Sallusto F (2009). Production of interleukin 22 but not interleukin 17 by a subset of human skin-homing memory T cells. Nat. Immunol 10, 857–863. [PubMed: 19578369]

Effros RB (1997). Loss of CD28 expression on T lymphocytes: a marker of replicative senescence. Dev. Comp. Immunol 21, 471–478. [PubMed: 9463780]

Glas AM, Knoops L, Delahaye L, Kersten MJ, Kibbelaar RE, Wessels LA, van Laar R, van Krieken JH, Baars JW, Raemaekers J, et al. (2007). Gene-expression and immunohistochemical study of specific T-cell subsets and accessory cell types in the transformation and prognosis of follicular lymphoma. J. Clin. Oncol 25, 390–398. [PubMed: 17200149]

Harrington LE, Hatton RD, Mangan PR, Turner H, Murphy TL, Murphy KM, and Weaver CT (2005). Interleukin 17-producing CD4+ effector T cells develop via a lineage distinct from the T helper type 1 and 2 lineages. Nat. Immunol 6, 1123–1132. [PubMed: 16200070]

Hendriks J, Gravestein LA, Tesselaar K, van Lier RA, Schumacher TN, and Borst J (2000). CD27 is required for generation and long-term maintenance of T cell immunity. Nat. Immunol 1, 433–440. [PubMed: 11062504]

Hilchey SP, Rosenberg AF, Hyrien O, Secor-Socha S, Cochran MR, Brady MT, Wang JC, Sanz I, Burack WR, Quataert SA, and Bernstein SH (2011). Follicular lymphoma tumor-infiltrating T-helper (T(H)) cells have the same polyfunctional potential as normal nodal T(H) cells despite skewed differentiation. Blood 118, 3591–3602. [PubMed: 21821704]

Hintzen RQ, Lens SM, Beckmann MP, Goodwin RG, Lynch D, and van Lier RA (1994). Characterization of the human CD27 ligand, a novel member of the TNF gene family. J. Immunol 152, 1762–1773. [PubMed: 8120385]

Hui E, Cheung J, Zhu J, Su X, Taylor MJ, Wallweber HA, Sasmal DK, Huang J, Kim JM, Mellman I, and Vale RD (2017). T cell costimulatory receptor CD28 is a primary target for PD-1-mediated inhibition. Science 355, 1428–1433. [PubMed: 28280247]

Kotecha N, Krutzik PO, and Irish JM (2010). Web-based analysis and publication of flow cytometry experiments. Curr. Protoc. Cytom Chapter 10, Unit10.17.

Laurent C, Müller S, Do C, Al-Saati T, Allart S, Larocca LM, Hohaus S, Duchez S, Quillet-Mary A, Laurent G, et al. (2011). Distribution, function, and prognostic value of cytotoxic T lymphocytes in follicular lymphoma: a 3-D tissue-imaging study. Blood 118, 5371–5379. [PubMed: 21856865]

Lee AM, Clear AJ, Calaminici M, Davies AJ, Jordan S, MacDougall F, Matthews J, Norton AJ, Gribben JG, Lister TA, and Goff LK (2006). Number of CD4+ cells and location of forkhead box protein P3-positive cells in diagnostic follicular lymphoma tissue microarrays correlates with outcome. J. Clin. Oncol 24, 5052–5059. [PubMed: 17033038]

Lee WW, Yang ZZ, Li G, Weyand CM, and Goronzy JJ (2007). Un-checked CD70 expression on T cells lowers threshold for T cell activation in rheumatoid arthritis. J. Immunol 179, 2609–2615. [PubMed: 17675524]

Lesokhin AM, Ansell SM, Armand P, Scott EC, Halwani A, Gutierrez M, Millenson MM, Cohen AD, Schuster SJ, Lebovic D, et al. (2016). Nivolumab in patients with relapsed or refractory hematologic malignancy: preliminary results of a phase Ib study. J. Clin. Oncol 34, 2698–2704. [PubMed: 27269947]

Maurer MJ, Bachy E, Ghesquières H, Ansell SM, Nowakowski GS, Thompson CA, Inwards DJ, Allmer C, Chassagne-Clément C, Nicolas-Virelizier E, et al. (2016). Early event status informs subsequent outcome in newly diagnosed follicular lymphoma. Am. J. Hematol 91, 1096–1101. [PubMed: 27465588]

Muenst S, Hoeller S, Willi N, Dirnhofera S, and Tzankov A (2010). Diagnostic and prognostic utility of PD-1 in B cell lymphomas. Dis. Markers 29, 47–53. [PubMed: 20826917]

Nograles KE, Zaba LC, Shemer A, Fuentes-Duculan J, Cardinale I, Kikuchi T, Ramon M, Bergman R, Krueger JG, and Guttman-Yassky E (2009). IL-22-producing “T22” T cells account for upregulated IL-22 in atopic dermatitis despite reduced IL-17-producing TH17 T cells. J. Allergy Clin. Immunol 123, 1244–1252.e2. [PubMed: 19439349]

Park H, Li Z, Yang XO, Chang SH, Nurieva R, Wang YH, Wang Y, Hood L, Zhu Z, Tian Q, and Dong C (2005). A distinct lineage of CD4 T cells regulates tissue inflammation by producing interleukin 17. Nat. Immunol 6, 1133–1141. [PubMed: 16200068]

Raimondi G, Shufesky WJ, Tokita D, Morelli AE, and Thomson AW (2006). Regulated compartmentalization of programmed cell death-1 discriminates CD4+CD25+ resting regulatory T cells from activated T cells. J. Immunol 176, 2808–2816. [PubMed: 16493037]

Richendollar BG, Pohlman B, Elson P, and Hsi ED (2011). Follicular programmed death 1-positive lymphocytes in the tumor microenvironment are an independent prognostic factor in follicular lymphoma. Hum. Pathol 42, 552–557. [PubMed: 21237493]

Schmidt D, Goronzy JJ, and Weyand CM (1996). CD4+ CD7- CD28-T cells are expanded in rheumatoid arthritis and are characterized by autoreactivity. J. Clin. Invest 97, 2027–2037. [PubMed: 8621791]

Simoni Y, Fehlings M, Kløverpris HN, McGovern N, Koo SL, Loh CY, Lim S, Kurioka A, Fergusson JR, Tang CL, et al. (2017). Human innate lymphoid cell subsets possess tissue-type based heterogeneity in phenotype and frequency. Immunity 46, 148–161. [PubMed: 27986455]

Tang Q, Henriksen KJ, Bi M, Finger EB, Szot G, Ye J, Masteller EL, McDevitt H, Bonyhadi M, and Bluestone JA (2004). In vitro-expanded antigen-specific regulatory T cells suppress autoimmune diabetes. J. Exp. Med 199, 1455–1465. [PubMed: 15184499]

Vallejo AN, Nestel AR, Schirmer M, Weyand CM, and Goronzy JJ (1998). Aging-related deficiency of CD28 expression in CD4+ T cells is associated with the loss of gene-specific nuclear factor binding activity. J. Biol. Chem 273, 8119–8129. [PubMed: 9525915]

Wahlin BE, Sander B, Christensson B, and Kimby E (2007). CD8+ T-cell content in diagnostic lymph nodes measured by flow cytometry is a predictor of survival in follicular lymphoma. Clin. Cancer Res 13, 388–397. [PubMed: 17255259]

Wahlin BE, Aggarwal M, Montes-Moreno S, Gonzalez LF, Roncador G, Sanchez-Verde L, Christensson B, Sander B, and Kimby E (2010). A unifying microenvironment model in follicular lymphoma: outcome is predicted by programmed death-1–positive, regulatory, cytotoxic, and helper T cells and macrophages. Clin. Cancer Res 16, 637–650. [PubMed: 20068089]

Wang L, Abbasi F, Ornatsky O, Cole KD, Misakian M, Gaigalas AK, He HJ, Marti GE, Tanner S, and Stebbings R (2012). Human CD4+ lymphocytes for antigen quantification: characterization using conventional flow cytometry and mass cytometry. Cytometry A 81, 567–575. [PubMed: 22539147]

Wogsland CE, Greenplate AR, Kolstad A, Myklebust JH, Irish JM, and Huse K (2017). Mass Cytometry of Follicular Lymphoma Tumors Reveals Intrinsic Heterogeneity in Proteins Including HLA-DR and a Deficit in Nonmalignant Plasmablast and Germinal Center B-Cell Populations. Cytometry B. Clin. Cytom 92, 79–87. [PubMed: 27933753]

Yang ZZ, Novak AJ, Stenson MJ, Witzig TE, and Ansell SM (2006). Intratumoral CD4+CD25+ regulatory T-cell-mediated suppression of infiltrating CD4+ T cells in B-cell non-Hodgkin lymphoma. Blood 107, 3639–3646. [PubMed: 16403912]

Yang ZZ, Novak AJ, Ziesmer SC, Witzig TE, and Ansell SM (2007). CD70+ non-Hodgkin lymphoma B cells induce Foxp3 expression and regulatory function in intratumoral CD4+CD25 T cells. Blood 110, 2537–2544. [PubMed: 17615291]

Yang ZZ, Novak AJ, Ziesmer SC, Witzig TE, and Ansell SM (2009). Malignant B cells skew the balance of regulatory T cells and TH17 cells in B-cell non-Hodgkin's lymphoma. Cancer Res. 69, 5522–5530. [PubMed: 19509224]

Yang ZZ, Grote DM, Ziesmer SC, Niki T, Hirashima M, Novak AJ, Witzig TE, and Ansell SM (2012). IL-12 upregulates TIM-3 expression and induces T cell exhaustion in patients with follicular B cell non-Hodgkin lymphoma. J. Clin. Invest 122, 1271–1282. [PubMed: 22426209]

Yang ZZ, Grote DM, Xiu B, Ziesmer SC, Price-Troska TL, Hodge LS, Yates DM, Novak AJ, and Ansell SM (2014). TGF-b upregulates CD70 expression and induces exhaustion of effector memory T cells in B-cell non-Hodgkin's lymphoma. Leukemia 28, 1872–1884. [PubMed: 24569779]

Yang ZZ, Grote DM, Ziesmer SC, Xiu B, Novak AJ, and Ansell SM (2015). PD-1 expression defines two distinct T-cell sub-populations in follicular lymphoma that differentially impact patient survival. Blood Cancer J. 5, e281. [PubMed: 25700246]

Yang ZZ, Kim HJ, Villasboas JC, Chen YP, Price-Troska T, Jalali S, Wilson M, Novak AJ, and Ansell SM (2017). Expression of LAG-3 defines exhaustion of intratumoral PD-1^{+} T cells and correlates with poor outcome in follicular lymphoma. Oncotarget 8, 61425–61439. [PubMed: 28977875]

Żabińska M, Krajewska M, Kościelska-Kasprzak K, and Klinger M (2016). CD3(+)CD8(+)CD28(−) T lymphocytes in patients with lupus nephritis. J. Immunol. Res 2016, 1058165. [PubMed: 27446964]

Highlights

- T cell profiles in the FL tumor microenvironment are distinct from control tissues
- Specific subsets of intratumoral T cells are associated with patient survival in FL
- Reduced expression of CD27 and CD28 represents a specific immune signature in FL

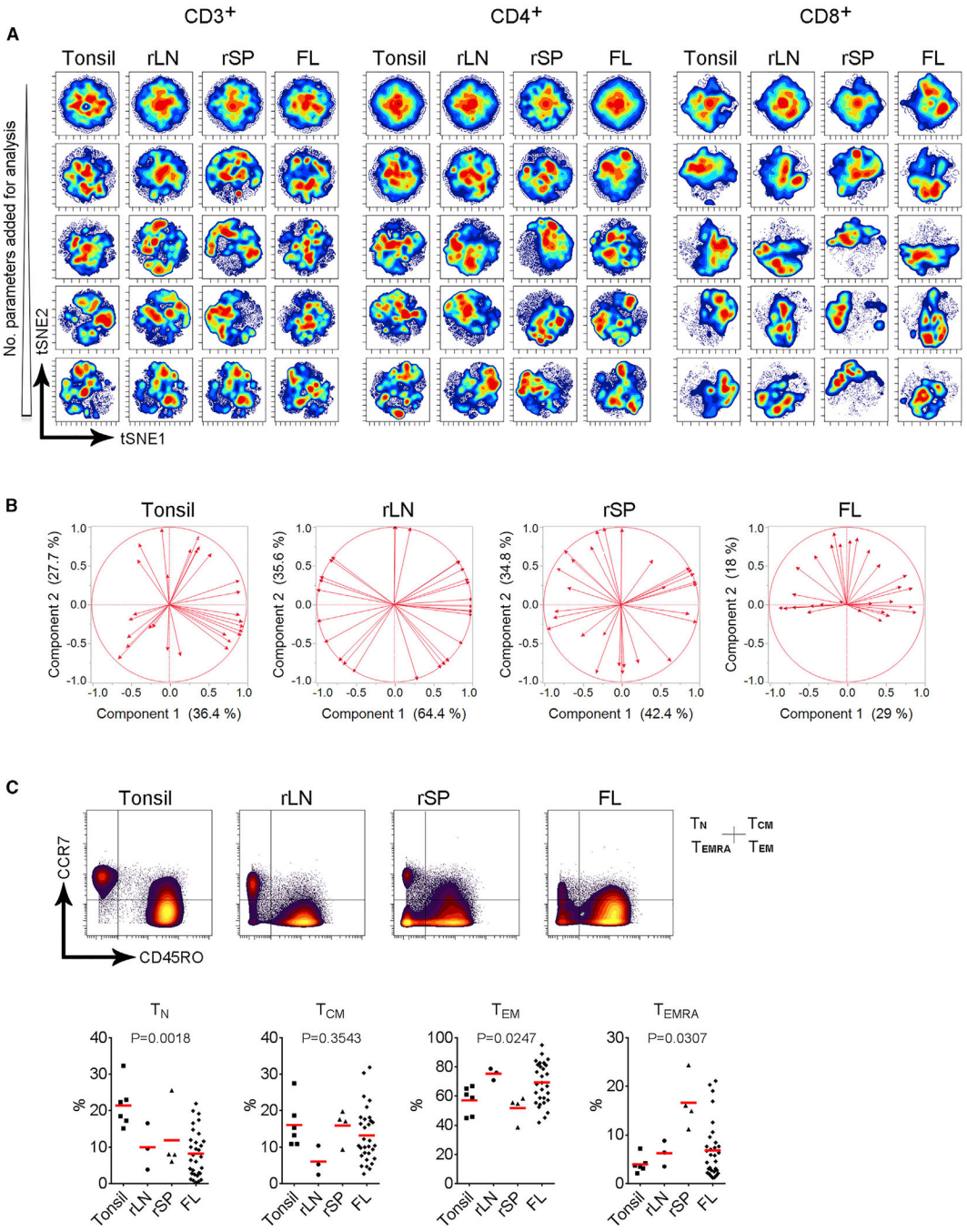

Figure 1. The Overall T Cell Profile in FL Patients Differs from Normal Controls

(A) The tSNE maps of $CD3^+$, $CD4^+$, and $CD8^+$ subsets from tonsil, reactive lymph node (rLN) and spleen (rSP) tissues, and FL biopsy specimens. The t-SNE analysis was performed on a concatenated file (31 FL, 6 tonsils, 3 rLNs, or 4 rSPs) using escalated parameter (surface makers).

(B) Plots of principal-component analysis of $CD3^+$ T cells from tonsil, rLN, rSP tissues, and FL biopsy specimens.

(C) Plots from a representative sample of tonsil, rLN, rSP, or FL showing expression of CD45RO and CCR7. Graphs show the percentages of naive, central memory, effector memory, and terminally differentiated T cells from $CD3^+$ T cells in tonsil, rLN, rSP, and FL. p value indicates a comparison between Tonsil and FL. See also Table S1 and Figures S1–S3.

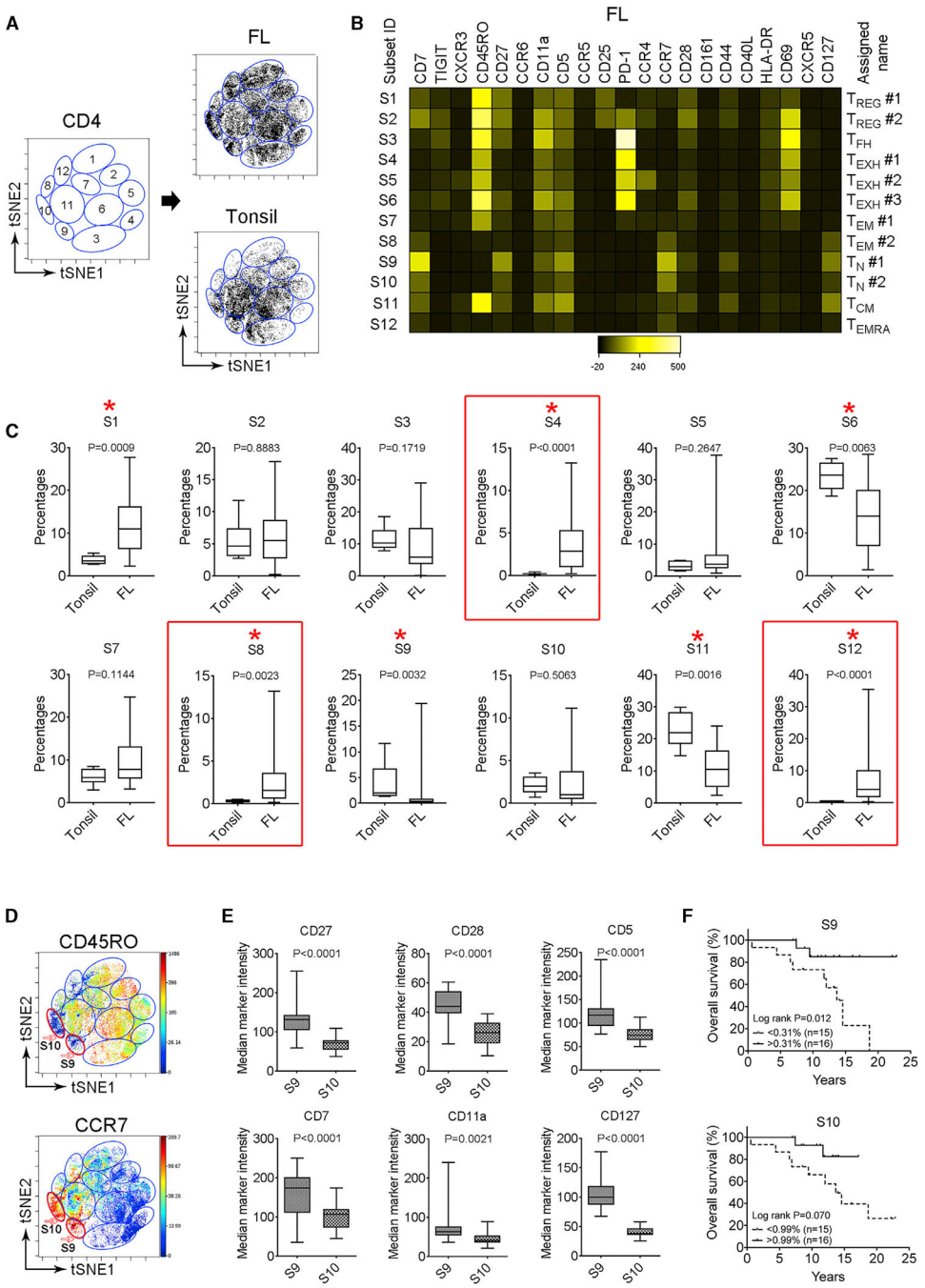

Figure 2. Multiple T Cell Subsets Are Present in Tumor Microenvironment of FL

(A) The tSNE maps of $CD4^+$ T cells from tonsil tissue and FL biopsy specimens. Clusters corresponding to different subsets circled with a number were identified by manual gating. Data shown were representative of one donor each from 31 FL and 6 tonsils.

(B) Heatmap showing median intensity of each marker for subsets identified above. Data shown were from donor represented in (A).

(C) Graphs showing the percentages of each subset in tonsil and FL. p value was calculated using nonparametric Mann-Whitney test; FL, n = 31; tonsil, n = 6.

(D) The tSNE maps of $CD4^+$ T cells from a representative FL specimen. CD45RO and CCR7 expression on subsets S9 and S10 in red circles was shown.
(E) Graphs showing the median marker intensity of surface markers from S9 or S10 in FL.
(F) Kaplan-Meier curves for overall survival of FL patients (n = 31) by the number of S9 or S10 with a cutoff of 0.31% or 0.99%, respectively.

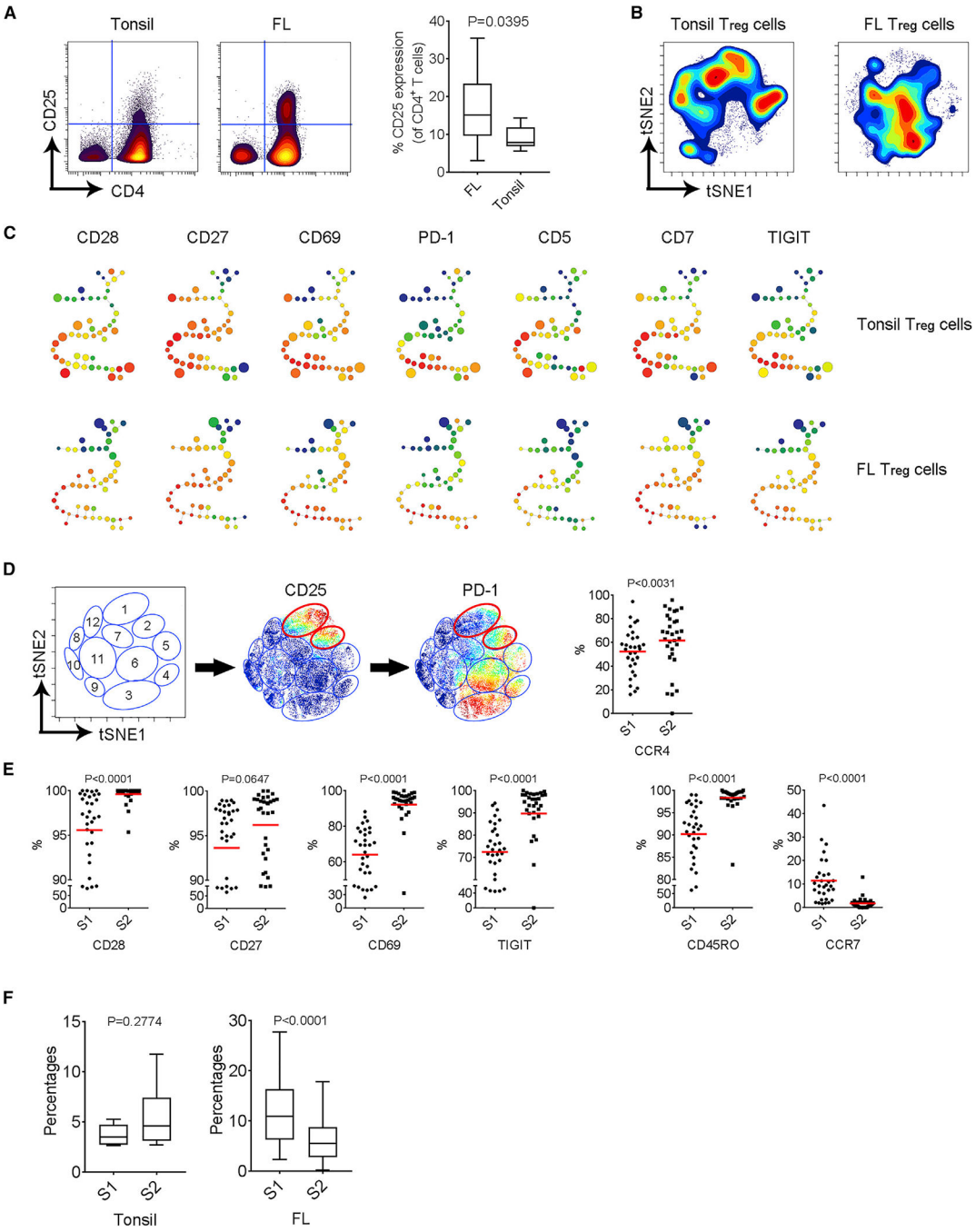

Figure 3. PD-1 Expression Distinguishes Activated T Cells from Intratumoral CD4$^+$CD25$^+$ T$_{reg}$ Cells

(A) Plots from a representative sample of tonsil and FL showing expression of CD25 on CD4$^+$ T cells. Graphs show the percentages of CD4$^+$CD25$^+$ T cells from 6 tonsil tissues and 31 FL specimens.

(B) The tSNE maps of CD4$^+$CD25$^+$ T cells from a concatenated file (31 FL or 6 tonsils).

(C) SPADE maps of CD4$^+$CD25$^+$ T cells from a concatenated file (31 FL or 6 tonsils). The dots in blue or in red indicate low or high expression, respectively. The dots with big size contain more cell events.

(D) The tSNE maps of $CD4^+$ T cells from a representative FL specimens. CD25 and PD-1 expression on subsets S1 and S2 in red circles was shown.
(E) Graphs showing the percentages of surface markers from S1 or S2 in FL.
(F) Graphs showing the percentages of S1 and S2 in tonsil and FL. p value was calculated using nonparametric Mann-Whitney test; FL, n = 31; tonsil, n = 6. See also Figure S4.

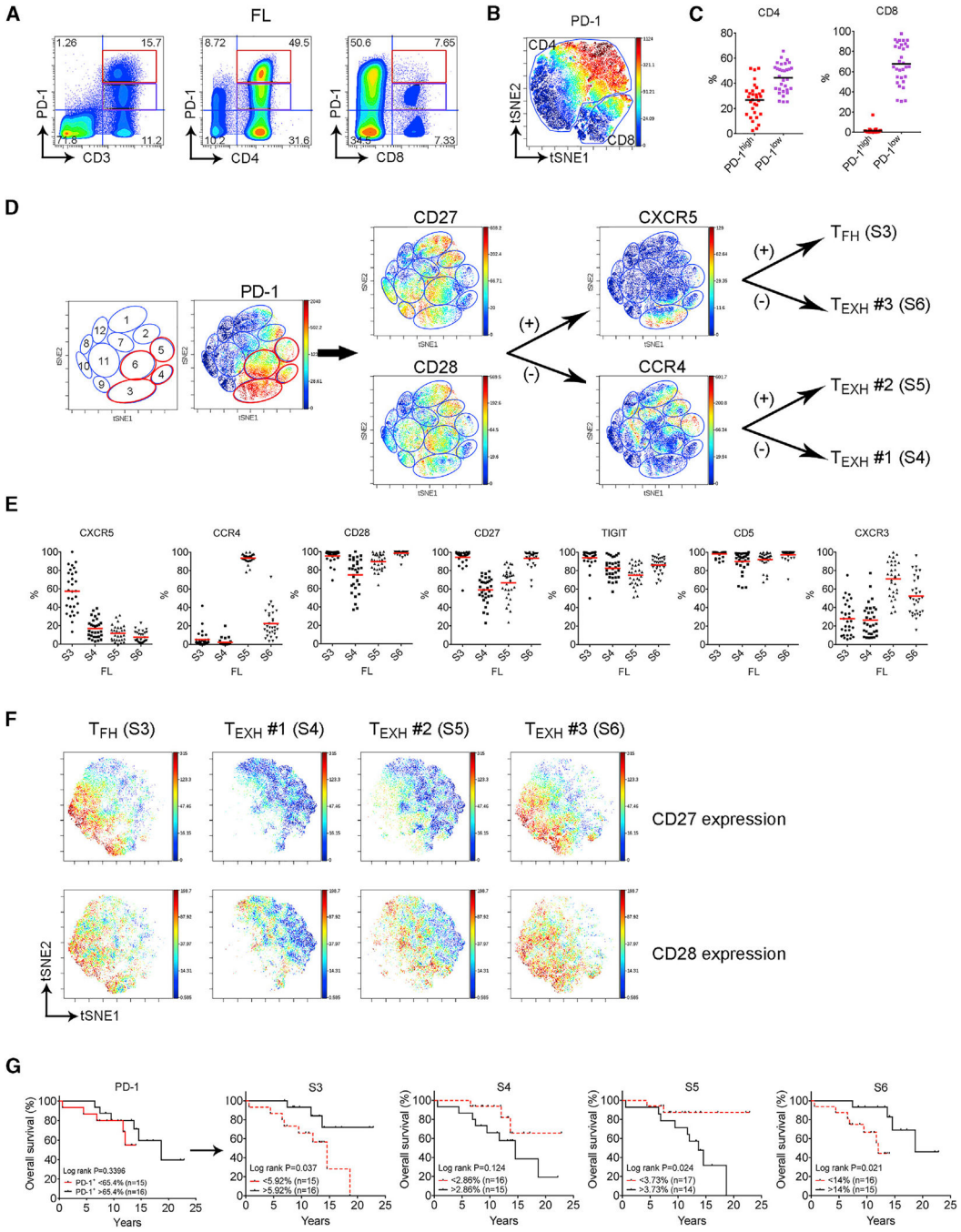

Figure 4. PD-1-Expressing T Cells Are Heterogeneous, and Subsets of PD-1$^+$ T Cells Are Associated with Overall Survival in FL

(A) Plots from a representative sample of FL showing expression of PD-1 on CD3$^+$, CD4$^+$, or CD8$^+$ T cells.

(B) The tSNE map of PD-1$^+$ cells from CD3$^+$ concatenated file (31 FL).

(C) Graphs showing the percentages of PD-1^{high} or PD-1^{low} cells from CD4$^+$ or CD8$^+$ T cells from 31 FL specimens.

(D) The tSNE maps of $CD4^+$ T cells from a representative FL specimen showing the gating strategy to identify $PD\text{-}1^+$ subsets (S3–S6). PD-1 expression on subsets S3–S6 in red circles was shown.

(E) Graphs showing the percentages of surface markers from S3, S4, S5, or S6 in FL.

(F) The tSNE maps of S3–S6 from the concatenated file of 31 FL specimens.

(G) Kaplan-Meier curves for overall survival of FL patients (n = 31) by the number of total $PD\text{-}1^+$ cells, S3, S4, S5, or S6 with a cutoff of 65.4%, 5.92%, 2.86%, 3.73%, or 14%, respectively. See also Figure S5.

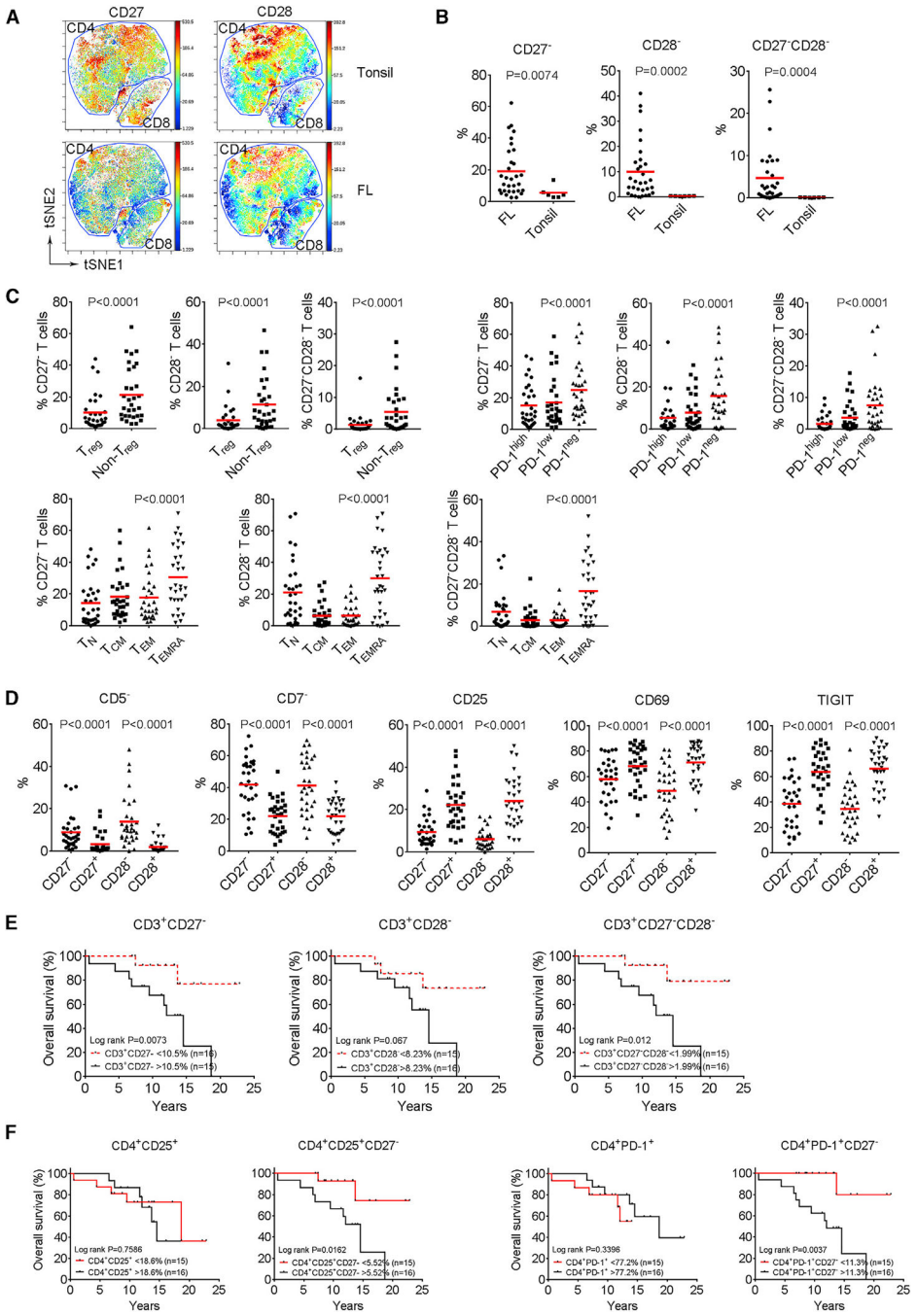

Figure 5. T Cells Deficient in Co-stimulatory Molecules Are Prevalent in FL and Predict Patient Outcome

(A) The tSNE map of CD27 or CD28^{+} cells from CD3^{+} concatenated file (31 FL and 6 tonsils). CD4^{+} or CD8^{+} T cells were gated based on expression levels from CD4 or CD8 staining.

(B) Graphs showing the percentages of CD27^{-} or CD28^{-} or CD27^{-}CD28^{-} cells from CD3^{+} T cells from 31 FL specimens and 6 tonsil tissues.

(C) Graphs showing the percentages of CD27^{-}, CD28^{-}, or CD27^{-}CD28^{-} cells from CD25^{-}, CD25^{+}, PD-1^{high}, PD-1^{low}, PD-1^{neg}, T_N, T_{CM}, T_{EM}, or T_{EMRA} cells from 31 FL specimens.

(D) Graphs showing the percentages of surface markers from $CD27^-$, $CD27^+$, $CD28^-$, or $CD28^+$ cells from 31 FL specimens.

(E and F) Kaplan-Meier curves for overall survival of FL patients (n = 31) by the number of $CD3^+CD27^-$, $CD3^+CD28^-$, $CD3^+CD27^-CD28^-$ (E), $CD4^+CD25^+$, $CD4^+CD25^+CD27^-$, $CD4^+PD\text{-}1^+$, or $CD4^+PD\text{-}1^+CD27^-$ (F) T cells. Bottom: p value indicates a comparison between T_N and T_{EMRA}. See also Figure S5.

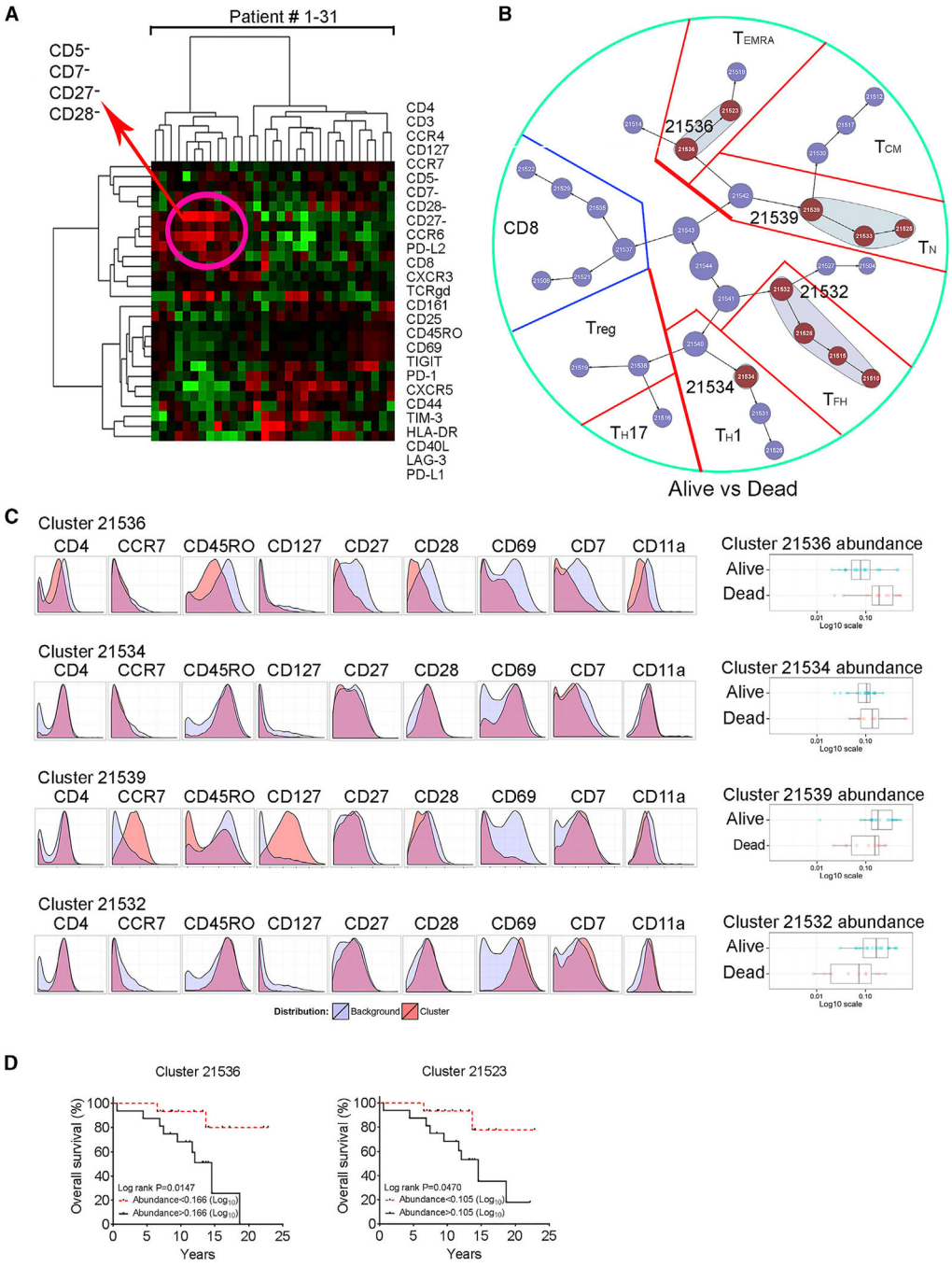

Figure 6. Loss of Co-stimulatory Receptor Expression Represents a Unique Immune Signature in FL

(A) Heatmap showing clustering results for differentially expressed markers on $CD3^+$ T cells from 31 FL specimens. Clustering was performed by Cluster 3.0 software. Each vertical column represents a patient sample.

(B) Plot showing clustering results from FL patients divided by 2 groups (alive versus dead). Circles in red represent clusters that differed between two groups. Number in circles indicates a cluster ID. Clustering was performed by CITRUS from Cytobank.

(C) Histogram plots in corners showing expression of selected markers by cells from 4 parent clusters overlapped to background. Expression level of each selected marker was expressed by Cluster (red) over Background (light blue). Graphs on the right showed quantitative results of abundance from 4 parent clusters between groups of Alive and Dead. The histograms and graphs were generated by CITRUS from Cytobank.
(D) Kaplan-Meier curves for overall survival of FL patients (n = 31) by the clusters 21536 and 21523 using a cutoff point of abundance. See also Figure S6.

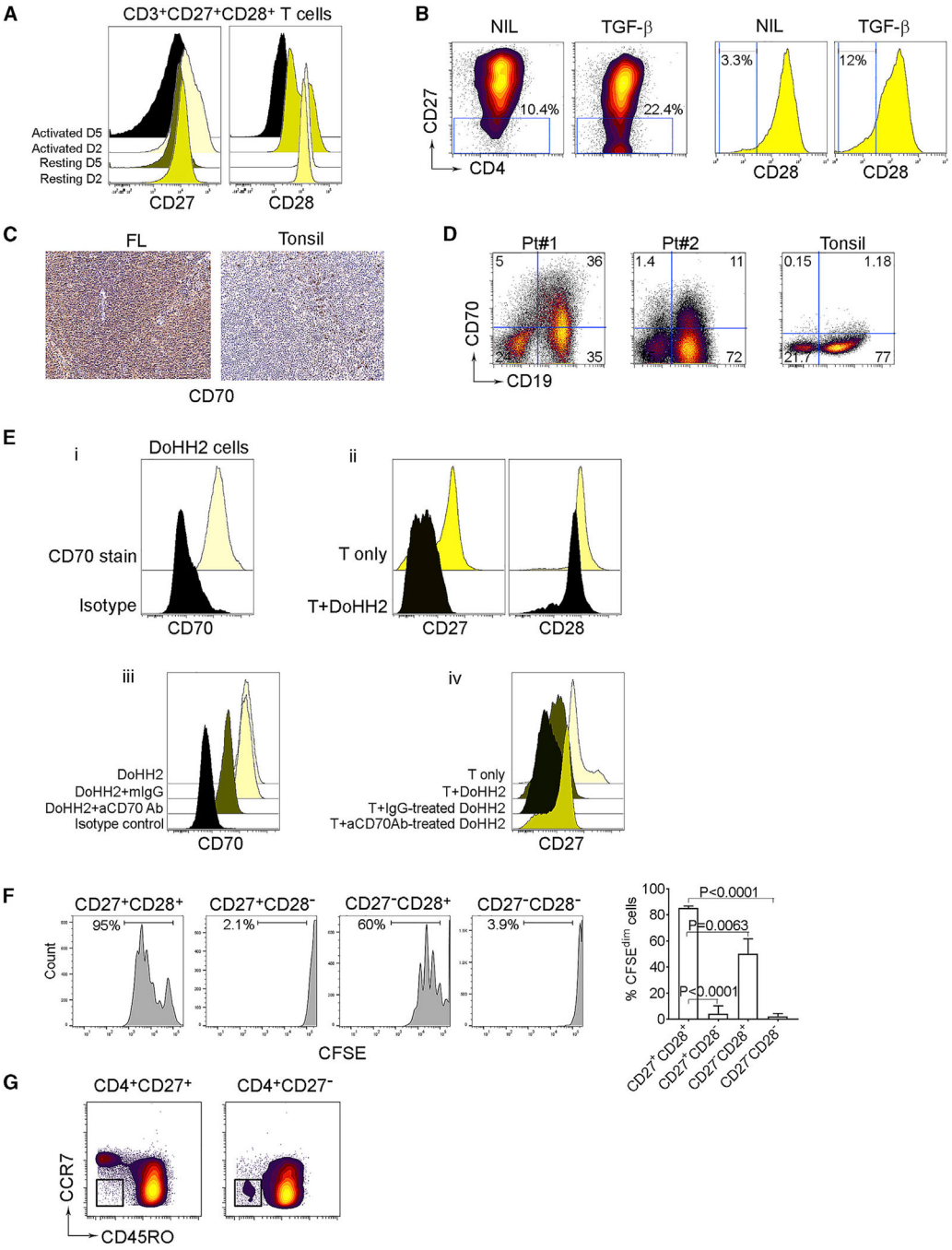

Figure 7. CD70^{+} Lymphoma Cells Induce Downregulation of CD27 or CD28 Expression on Intratumoral T Cells, which Impairs Their Capacity to Proliferate

(A) Histograms showing CD27 or CD28 expression of CD27^{+}CD28^{+} T cells cultured in anti-CD3-coated plate plus anti-CD28 Ab for 2 or 5 days (activated). Cells cultured in uncoated plate were used as control (resting).

(B) CD27 or CD28 expression from CD4^{+} T cells cultured in anti-CD3-coated plate plus anti-CD28 Ab in the presence or absence of TGF-β for 3 days.

(C) Immunohistochemistry showing CD70 expression from FL (n = 8) and tonsil tissue.

(D) Plots showing CD70 expression on $CD19^+$ cells from representative lymphoma (n = 11) and tonsil tissues.

(E) Histograms showing (i) CD70 expression on DoHH2 cells, (ii) expression of CD27 and CD28 on T cells co-cultured with DoHH2 cells for 3 days, (iii) CD70 expression of DoHH2 cells treated with either anti-CD70 blocking Ab or mIgG for 2 h, and (iv) expression of CD27 on $CD4^+$ T cells co-cultured with DoHH2 cells pretreated with either anti-CD70 blocking Ab or mIgG for 3 days.

(F) Histograms showing CFSE staining of $CD27^+CD28^+$, $CD27^+CD28^-$, $CD27^-CD28^+$, or $CD27^-CD28^-$ T cells cultured in anti-CD3-coated plate plus anti-CD28 Ab for 3 days. Graph shows the numbers of $CFSE^{dim}$ cells of these subsets; n = 4.

(G) Plots showing CD45RO and CCR7 expression from $CD4^+CD27^-$ or $CD4^+CD27^+$ T cells. Cells in box represent terminally differentiated T cells ($CD45RO^-CCR7^-$; T_{EMRA}). See also Figure S7.

KEY RESOURCES TABLE

REAGENT or RESOURCE	SOURCE	IDENTIFIER
Antibodies		
Antibodies for CyTOF assay	Fluidigm	https://www.fluidigm.com/. See also Table S1
Mouse anti-CD3 (OKT3)	eBioscience	Cat#:14-0037-82; RRID:AB_467057
Mouse anti-CD3, V500	BD	Cat#:561416; RRID:AB_10612021
Mouse anti-CD4, APC-H7	BD	Cat#:560158; RRID:AB_1645478
Mouse anti-CD27, PE/Cy7	Biolegend	Cat#:302838; RRID:AB_2561919
Anti-CD28, pure, low azide (0.01%)	BD	Cat#:340975; RRID:AB_400197
Mouse anti-CD28, PE	Biolegend	Cat#:302908; RRID:AB_314310
Rabbit anti-CD70,	Lifespan Bioscience	Cat#:LS-A8809; RRID:AB_11190041
Mouse anti-CD70, PE	BD	Cat#:555835; RRID:AB_396158
Mouse anti-CD19, Percp	BD	Cat#:347544; RRID:AB_400321
Mouse anti-PD-1, Percp-Cy5.5	BD	Cat#:561273; RRID:AB_10645786
EasySep Human CD3 Positive Selection Kit II	StemCell	Cat#:17851RF
EasySep Human CD4 Positive Selection Kit II	StemCell	Cat#:17852RF
Biological samples		
FL patient biopsy specimens	Mayo Clinic	The use of human tissue samples for this study was approved by the Institutional Review Board of the Mayo Clinic. See Table S2
Chemicals, Peptides, and Recombinant Proteins		
Reagents for CyTOF assay	Fluidigm	https://www.fluidigm.com/
Fc Receptor Blocking Solution	Biolegend	Cat#:422301
CFSE	Sigma	Cat#:150347-59-4
Ficoll-Paque PLUS	GE Healthcare	Product code#:17-1440-03
Recombinant human TGF-β1	PeproTech	Cat#:100-21
Experimental Models: Cell Lines		
Raji	ATCC	ATCC#:CCL-86
DoHH2	DSMZ	DSMZ#:ACC 47
Mec-1	DSMZ	DSMZ#:ACC 497
Software and Algorithms		
Cytobank	Cytobank	https://premium.cytobank.org/cytobank/
viSNE	Cytobank	https://premium.cytobank.org/cytobank/
CITRUS	Cytobank	https://premium.cytobank.org/cytobank/
SPADE	Cytobank	https://premium.cytobank.org/cytobank/
Prism 7	GraphPad Software	https://www.graphpad.com/
Photoshop CC	Adobe Systems	N/A
Cluster 3.0	Java TreeView 1.0.5	http://bonsai.hgc.jp/~mdehoon/software/cluster/software.htm
Deposited Data		
CyTOF files	FlowRepository	http://flowrepository.org/